Plant Physiol. (1989) 89, 197–203
0032-0889/89/89/0197/07/$01.00/0

Received for publication June 10, 1988
and in revised form August 15, 1988

Observation of Cytoplasmic and Vacuolar Malate in Maize Root Tips by ^{13}C-NMR Spectroscopy[1]

Keejong Chang and Justin K. M. Roberts*

Department of Biochemistry, University of California, Riverside, California 92521

ABSTRACT

The accumulation of malate by maize (*Zea mays* L.) root tips perfused with $KH^{13}CO_3$ was followed by ^{13}C nuclear magnetic resonance spectroscopy. *In vivo* nuclear magnetic resonance spectra contained distinct signals from two pools of malate in maize root tips, one at a pH ~5.3 (assigned to the vacuole) and one at a pH > 6.5 (assigned to the cytoplasm). The ratio of cytoplasmic to vacuolar malate was lower in 12 millimeter long root tips than in 2 millimeter root tips. The relatively broad width of the signals from C1- and C4-labeled vacuolar malate indicated heterogeneity in vacuolar pH. During the 3 hour $KH^{13}CO_3$ treatment, ^{13}C-malate accumulated first primarily in the cytoplasm, increasing to a fairly constant level of ~6 millimolar by 1 hour. After a lag, vacuolar malate increased throughout the experiment.

Malate plays a prominent role in many metabolic processes in plants, such as ion transport and carbohydrate metabolism (see Ref. 11 for review). Attempts to understand these processes are complicated by the existence of metabolically distinct pools of malate in plant cells (12–14). In maize roots, the relative amount of malate that is out of equilibrium with respiratory processes is much higher in cells with a greater vacuolar volume (14). Quantitative knowledge of the compartmentation of malate is a prerequisite to an understanding of the transport of malate across the tonoplast, and the regulation of enzymes involved in the metabolism of malate. To date, this transport and these enzymes have been examined primarily *in vitro* (2, 6, 16); information on the concentrations of malate that these proteins experience *in vivo* is limited. Gerhardt and Heldt (4) were able to obtain a rough estimate of cytoplasmic malate concentrations in spinach leaves, by fractionating frozen leaves in nonaqueous media. They found the concentration of cytoplasmic malate to be <1 mM in the dark, and <2.5 mM in the light.

NMR spectroscopy has been used to observe metabolites, conditions and compartmentation in plant cells (15, 20, 21). The method permits biochemical phenomena in plants to be examined without extrapolation from plant extracts. Stidham *et al.* (26) used ^{13}C-NMR to observe the incorporation of $^{13}CO_2$ into malate by leaves exhibiting CAM. The positions (*i.e.* chemical shifts) of signals from C4 and C1 carboxyls of malate are pH sensitive, and so were used as pH indicators, enabling measurement of the low vacuolar pHs. No signals were detected from malate pools experiencing near-neutral pHs, approximating the cytoplasmic pH of plant cells (22). This result was attributed to the small proportion of the cells occupied by cytoplasm in leaves of CAM plants (26). The cells that make up root apices contain a large proportion of cytoplasm (25) and so are particularly suited for studies of primary metabolism. Here we show that ^{13}C-NMR spectroscopy can be used to monitor cytoplasmic and vacuolar pools of malate in maize root tips.

MATERIALS AND METHODS

Maize (*Zea mays* L.; Funk hybrid 4323 from Germain's Seeds, Los Angeles, CA) was soaked for 1 d in flowing deionized water, then covered with wet paper towels in a tray. After ~48 h, root tips (either 2 or 12 mm long) were excised on ice with a razor blade. Each NMR sample contained ~2.5 g of root tips. After transfer to a 10 mm NMR tube modified to permit perfusion (19), root tips were perfused with oxygen-saturated 5 mM glucose plus 0.1 mM $CaSO_4$ for about 1 h. Then 5 mM $KHCO_3$, derived from 5 mM K_2CO_3 brought to pH 7.3 with 3-(*N*-morpholino)propanesulfonic acid was added: ^{13}C-labeled (Merck, Montreal, Canada) except for natural abundance ^{13}C-NMR and ^{31}P experiments. Thus, bicarbonate solutions contained 5 mM $KHCO_3$, 5 mM potassium 3-(*N*-morpholino)propanesulfonate, and ~5 mM 3-(*N*-morpholino)propanesulfonic acid.

Fourier transform NMR ^{13}C and ^{31}P spectra were obtained using a General Electric GN-500 spectrometer operating at 125.7 and 202.5 MHz, respectively. The ^{13}C-NMR spectra were obtained with bilevel proton decoupling using the WALTZ pulse sequence. The interval between 40° pulses was ~2.4 s (spectra of carboxyl groups were unchanged when a pulse interval of 15 s was employed); spectral width 30,000 Hz, 16K data points. ^{13}C-Chemical shifts were referenced to the combined resonance from the αC1 of glucose and the αC1 of the glucose moiety in sucrose, both at 93 ppm. Twenty Hz line broadening was applied to spectra prior to Fourier transformation. Resolution enhancement (Fig. 1C) of spectra was achieved by double exponential multiplication (using standard GE software, DM = 15) of data prior to Fourier transformation (3). ^{31}P NMR spectra were obtained with a pulse interval of 1.5 s; spectral width 8,000 Hz, 8K data points. Fifteen Hz line broadening was applied to spectra prior to Fourier transformation. Experiments were run at room temperature.

At the end of NMR experiments, samples were frozen in liquid nitrogen. Low mol wt metabolites were extracted from

[1] This work was made possible by grants from the National Science Foundation (DMB 8521564-01 and DMB 8604091), The Department of Energy (FG03-86FR13535), and the National Institutes of Health (PHS BRSG 2 507).

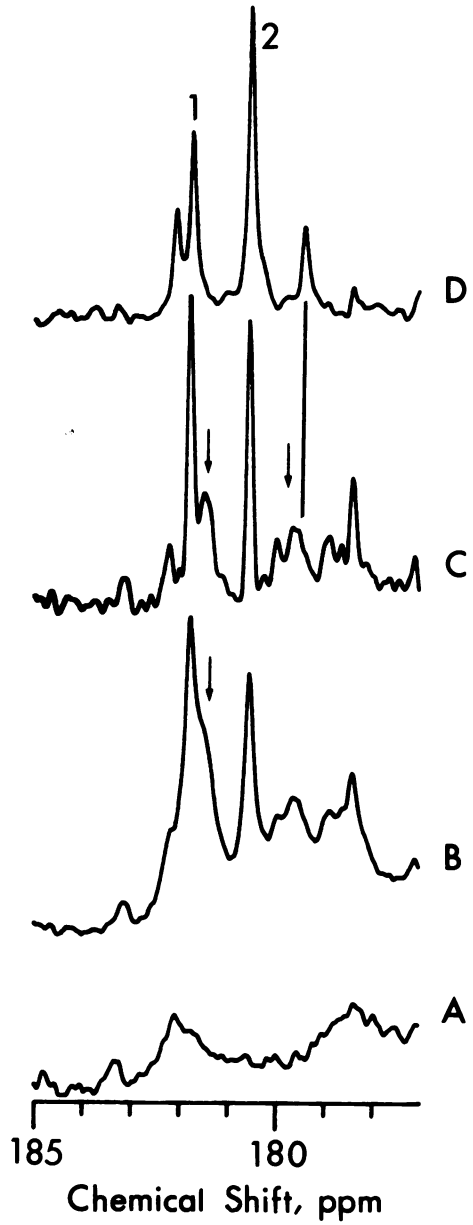

Figure 1. ^{13}C-NMR spectra of carboxylic acid groups in 2 mm long maize root tips and root tip extracts. A, Natural abundance spectrum of 2 mm long root tips perfused with oxygen-saturated 5 mM glucose, 5 mM $KH^{12}CO_3$, and 0.1 mM $CaSO_4$ for 3 h; B, same as (A) except root tips perfused with 5 mM $KH^{13}CO_3$; C, 'resolution enhanced' spectrum, obtained from the same free induction decay used to generate spectrum (B), using double exponential multiplication (DM = 15) according to Ferrige and Lindon (3); D, spectrum of extract of root tips giving spectrum (B), pH 7.5. Peak assignments: 1, C1 of malate; 2, C4 of malate; the arrows indicate signals from vacuolar malate (left, C1; right, C4). The peak to the left of peak 1 in (D), and the peak to the right of peak 2 (identified with the vertical line), are tentatively assigned to aconitate.

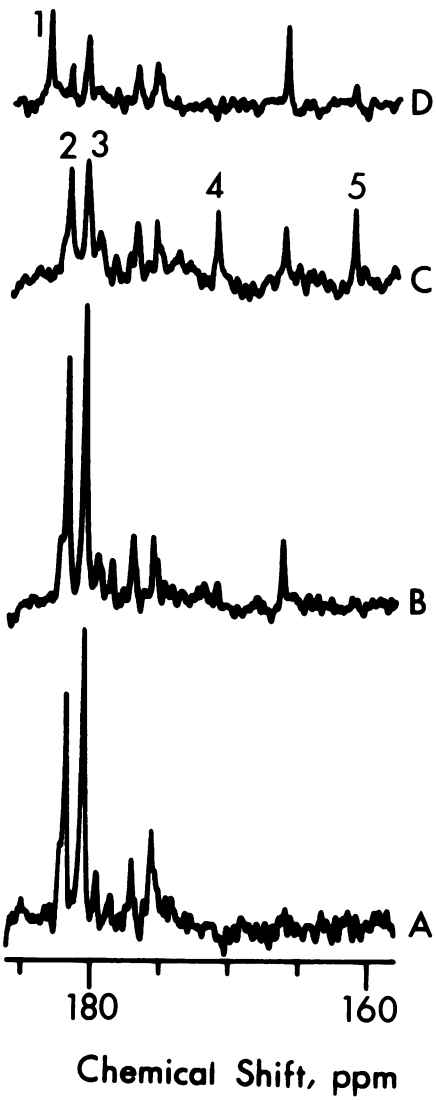

Figure 2. Identification of ^{13}C-NMR signals from the carboxylic acid groups of malate. A, Spectrum of extract of 2 mm long root tips after exposure to oxygen-saturated 5 mM $KH^{13}CO_3$, 5 mM Glc, and 0.1 mM $CaSO_4$ for 3 h; B, spectrum of same sample giving spectrum (A), after addition of NADP to a final concentration of 12 mM; C, spectrum of same sample giving spectrum (B), after addition of 0.3 units/mL of malic enzyme; D, spectrum of same sample giving spectrum (C), after bubbling 10 min with N_2 (to remove CO_2 and HCO_3^-) and addition of NADH to a final concentration of 6 mM, and 2 units/mL of lactate dehydrogenase. Addition of NADH and lactate dehydrogenase, alone, to root tip extracts had no effect on malate signals (data not shown). Peak assignments: 1, C1 of lactate (present only in spectrum D); 2, C1 of malate; 3, C4 of malate; 4, C1 of pyruvate; 5, HCO_3^-.

the samples with 5% $HClO_4$, followed by centrifugation and neutralization with KOH. Proton-decoupled ^{13}C-NMR spectra of extracts at different pHs were obtained as described above. Total malate in root tip extracts was assayed enzymically (5). Enzymes and chemicals were obtained from Sigma Chemical Co. (St. Louis, MO) or U.S. Biochemical Co. (Cleveland, OH). Time courses for total malate accumulation were obtained by assaying extracts from individual samples of ~20 root tips, 2 mm long. The individual samples were placed in a holder consisting of a disposable 200 μL plastic pipette tip containing a coarse plastic mesh plug. Several of these samples were strung together, the samples being perfused in series. At appropriate times during the 3 h experiment, samples were removed and frozen in liquid nitrogen, prior to extraction and assay.

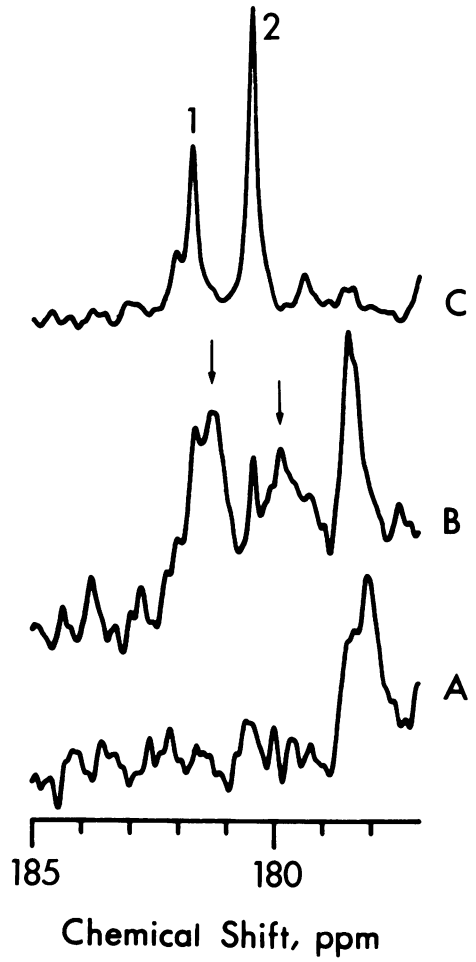

Figure 3. ^{13}C-NMR spectra of carboxylic acid groups in 12 mm maize root tips and root tip extracts. A, Natural abundance spectrum of 12 mm root tips exposed to $KH^{12}CO_3$ for 3 h as in Figure 1A; B, spectrum of 12 mm maize root tips labeled with $KH^{13}CO_3$ for 3 h; C, spectrum of extract of roots in (B), pH 7.5. Peak assignments: 1, C1 of malate; 2, C4 of malate; the arrows indicate signals from vacuolar malate (left, C1; right, C4).

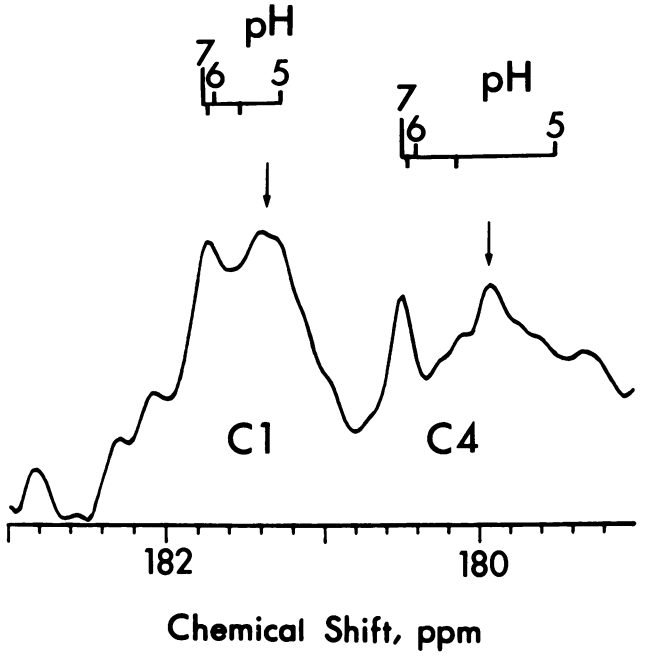

Figure 4. Heterogeneity of vacuolar pH in maize root tips demonstrated by *in vivo* ^{13}C-NMR. NMR spectrum is of 12 mm root tips treated with $KH^{13}CO_3$ (same spectrum as Fig. 3B). The two scales indicate the chemical shifts of C1 (left) and C4 (right) malate resonances from pH 5 to pH 7, determined by titration of extracts (*cf.* Fig. 3C). The arrows indicate signals from vacuolar malate (left, C1; right, C4).

RESULTS AND DISCUSSION

Carbon-13 NMR spectra of 2 mm long maize root tips treated with 5 mM $KH^{13}CO_3$ show strong signals from carboxylic acid groups (Fig. 1B), relative to spectra of unlabeled root tips (Fig. 1A). Perchloric acid extracts of unlabeled root tips gave no detectable ^{13}C-NMR signals characteristic of carboxylic acid groups (data not shown), indicating that the broad *in vivo* signals shown in Figure 1A are due to carboxylic acid groups on macromolecules that are removed by perchloric acid extraction. In contrast, spectra of extracts of root tips treated with ^{13}C-bicarbonate show clear signals from carboxylic acid groups, with signals from C4 and C1 of malate dominating the spectra (Fig. 1D). Peaks 1 and 2 in Figure 1D are assigned to C1 and C4 of malate, respectively, because (a) the chemical shifts match those of pure malate over a wide pH range (*cf.* 15, 26); (b) the intensities of peaks 1 and 2 are selectively reduced when malic enzyme and NADP are added to the extract (Fig. 2); (c) under the experimental conditions described in Figure 1B, root tips accumulate several μmol of malate per g fresh weight (data presented below)—quantities of ^{13}C-malate that are readily detectable by high resolution ^{13}C-NMR. C4-labeled malate is the product of carboxylation via PEP carboxylase, followed by action of malate dehydrogenase (7, 27); C1-labeled malate will be produced by randomization of C1 and C4 by mitochondrial fumarase (17).

The two smaller peaks on either side of the malate signals in Figure 1D are tentatively assigned to C1 and C6 of aconitate. While malate is generally the organic acid in maize root tips labeled most by exogenous $H^{13}CO_3^-$, under some conditions accumulation of labeled aconitate can rival that of malate; for example, compare results of Splittstoesser (24) with those of Ting and Dugger (27). We found that the nonmalate peaks were much stronger in root tips treated with ^{13}C-bicarbonate in the presence of 5 mM K_2SO_4 (data not shown); such treatments were avoided in this study.

The two strongest signals of the *in vivo* ^{13}C-NMR spectrum (Fig. 1B) have chemical shifts identical to the two malate signals from the root tip extract at pH 7.5 (peaks 1 and 2 in Fig. 1D). The chemical shifts of the carboxylic acid groups of malate are relatively insensitive to pHs above ~6.5 (26). Cytoplasm occupies most of the extravacuolar space in root tips (25) and is near neutral while the vacuole is acidic (22). Hence, we conclude that the malate responsible for peaks 1 and 2 is predominantly cytoplasmic. While mitochondria occupy only ~10% of the volume of the cytoplasm (25), the existence of significant quantities of C1-labeled malate indicates that much of the malate synthesized in root tips at some point passes into the mitochondria, where fumarase will randomize malate carbons (17).

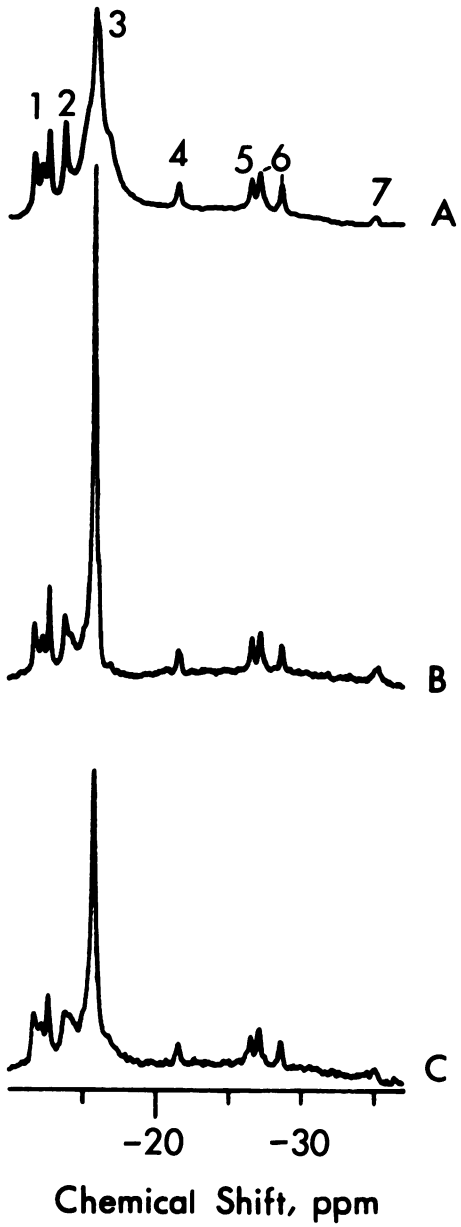

Figure 5. Suppression of vacuolar resonances by sequestration of Mn^{2+} in vacuoles: ^{31}P-NMR spectra of maize root tips *in vivo*. A, 2 mm long root tips treated with oxygen-saturated 5 mM glucose, 5 75mM $KHCO_3$, and 0.1 mM $CaSO_4$; 4h spectrum; B, 12 mm long root tips perfused as in (A); 2 h spectrum; C, 12 mm long root tips were treated with same solution as in (A) plus 0.2 mM Mn^{2+}, 2 h spectrum, 2 to 4 h after addition of Mn^{2+}. Peak assignments: 1, Glc-6-P; 2, cytoplasmic Pi; 3, vacuolar Pi; 4, 5 and 7, nucleoside triphosphate; 6, UDP-Glc and nicotinamide adenine nucleotides.

Upfield of the sharp cytoplasmic malate signals in Figure 1B are resonances (identified with arrows) that have chemical shifts not found in the spectrum of a neutral extract: a shoulder on peak 1, visible as a distinct peak in the resolution enhanced spectrum (Fig. 1C), and a broad signal to the right of peak 2, which does not correspond to any peak in Figure 1D. We assign these two resonances to vacuolar malate based on the following observations. The pH of the vacuoles of maize root tips has been estimated to be ~5.5 using ^{31}P-NMR

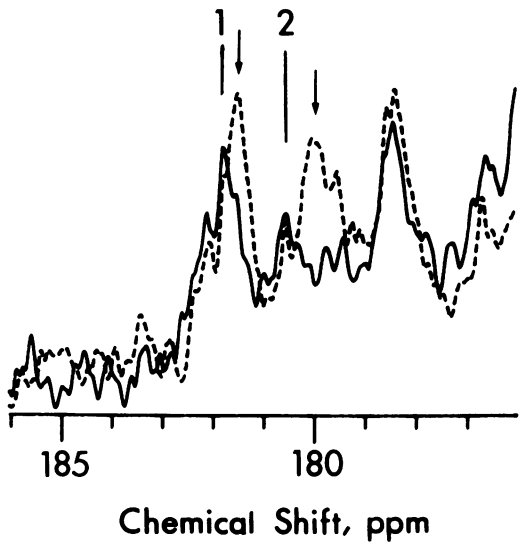

Figure 6. Suppression of vacuolar resonances by sequestration of Mn^{2+} in vacuoles: ^{13}C-NMR spectra of 12 mm long maize root tips *in vivo*. Root labeled with $KH^{13}CO_3$ in the presence (——) or absence (– – –) of 0.2 mM Mn^{2+}; spectra acquired 2 to 5 h after addition of $KH^{13}CO_3$. Peak assignments: 1, C1 of malate in cytoplasm; 2, C4 of malate in cytoplasm. The arrows indicate signals from vacuolar malate (left, C1; right, C4).

(22), this method having an uncertainty of a few tenths of a pH unit in this pH range (23). When the extract is acidified to ~pH 5.3 (which causes all the signals to move upfield to lower chemical shift values as the carboxylic acid groups protonate), the two malate signals have chemical shifts similar to these *in vivo* resonances.

The incorporation of ^{13}C-label into the C1-position of malate is ~60% of that into C4 (Fig. 1D). At first glance, *in vivo* spectra of labeled root tips suggest that labeling into C1 is greater than that into C4 (Fig. 1, B and C; peak 1 > peak 2). This difference is not due to saturation effects, for the relative intensities of the peaks in both spectra were unchanged when the pulse interval was increased from the usual 2.4 s to 15 s (data not shown). We attribute the difference first to the contribution of a broad signal at ~182 ppm in tissue spectra due to macromolecules, which is visible in the natural abundance ^{13}C-NMR spectrum of root tips (Fig. 1A). As noted above, this broad signal is lost upon extraction. Second, the carboxylic acid group giving a signal to the left of peak 1 in the spectrum of the neutral extract (chemical shift ~182 ppm in Fig. 1D), contributes to the intensity of peak 1 *in vivo* (Fig. 1, B and C). Note that the intensity of the signal just to the left of peak 1 is significantly smaller *in vivo* (Fig. 1, B and C) than *in vitro* at near-neutral pH (Fig. 1D), indicating that most of this organic acid is not in the cytoplasm. At pH 5.3, which approximates to the vacuolar pH, this smaller peak has a chemical shift identical to that of the C1 of malate at neutral pH (data not shown). Third, the signals from C1-malate in cytoplasm and vacuole partially overlap, increasing the height of peak 1, while C4 signals from the two pools of malate give separate signals (Fig. 1C). This result is due to the higher pK_a of the carboxylic acid group at C4, relative to C1. When the contributions of nonmalate signals are subtracted, the ratio

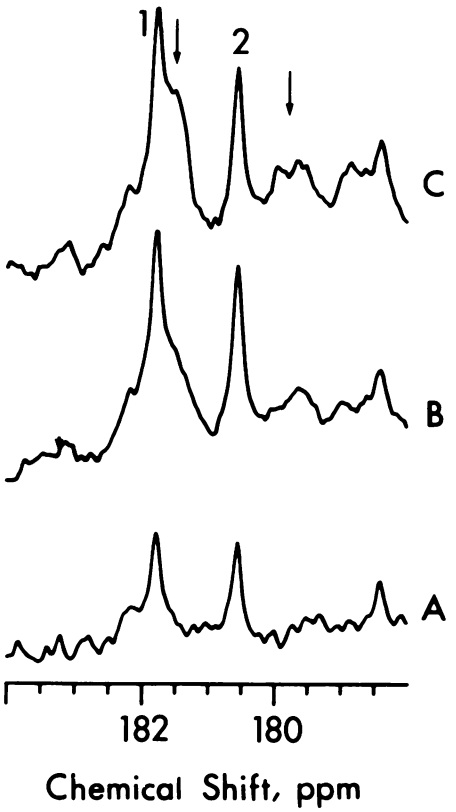

Figure 7. Changes in ^{13}C-NMR spectra of 2 mm long maize root tips during perfusion with $KH^{13}CO_3$. Roots were treated with oxygen-saturated 5 mM glucose, 5 mM $KH^{13}CO_3$, 0.1 mM $CaSO_4$ for 3 h. Spectra were acquired during first (A), second (B), and third (C)h of treatment. Peak assignments: 1, C1-malate in cytoplasm; 2, C4-malate in cytoplasm; the arrows indicate signals from vacuolar malate (left, C1; right, C4).

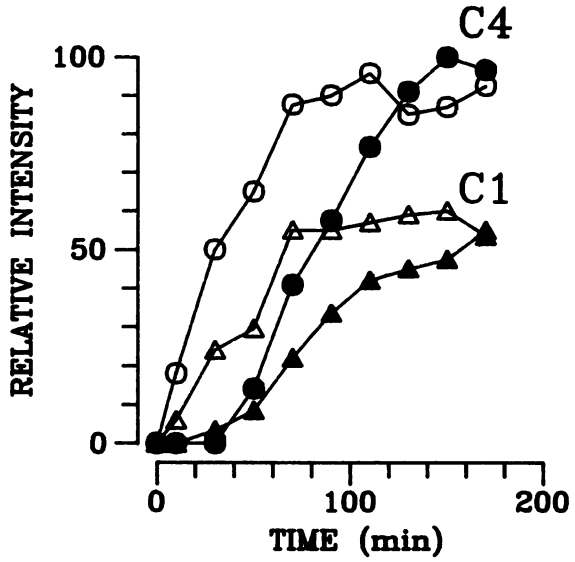

Figure 8. Accumulation and compartmentation of ^{13}C-malate in 2 mm maize root tips. Relative intensities of signals (proportional to concentrations) from the C4 (circles) and C1 (triangles) of ^{13}C-malate; open symbols represent cytoplasmic malate; closed symbols, vacuolar malate. Data were obtained by integrating (cutting and weighing) peak areas from spectra obtained every 20 min (spectra from two identical experiments were combined). The area of the C1 malate signals were determined after subtracting contributions apparent in the natural abundance spectrum (*cf.* Fig. 1A) and from a nonmalate carboxylic acid group (peak to the left of peak 1 in Fig. 1D).

Table I. *Concentration of Cytoplasmic Malate in 2 mm Maize Root Tips During Exposure to $KH^{13}CO_3$*

The percent ^{13}C-malate in the cytoplasm was determined using data in Figure 8. Total malate was determined by enzymic assay of extracts; the initial malate content was 3 μmol/g fresh weight. The concentration of cytoplasmic malate was estimated assuming complete equilibration of ^{13}C- and ^{12}C-malate, and a cytoplasmic volume 65% of total cell volume.

Time	^{13}C-Malate in Cytoplasm	Total Malate Content	[Malate] in Cytoplasm
min	*% of total*	*μmol/g fr wt*	*mM*
50	80.7	5.0	6.2
110	55.7	6.6	5.7
170	49.1	7.3	5.5

of C1 to C4 malate (vacuolar plus cytoplasmic) determined *in vivo* is comparable to that *in vitro*.

When 12 mm root tips treated with $KH^{13}CO_3$ were examined using ^{13}C-NMR (Fig. 3B), the intensities of the signals from C1 and C4 carboxyls of vacuolar malate were comparable to those from cytoplasmic malate. Thus, in long root tips, relatively more malate is partitioned into vacuoles than in shorter root tips (compare Figs. 3B and 1B) during a 3 h $KHCO_3$ treatment. This result may reflect the greater proportion of the cell volume occupied by vacuoles in the older tissue of the longer root tips.

If root tip vacuoles containing malate were of slightly different pHs, a broad vacuolar malate peak would result, arising from multiple overlapping resonances. Hence, the broad line-widths of the signals from vacuolar malate suggest heterogeneity in vacuolar pH. For example, in Figure 4, peaks 1 and 2 due to cytoplasmic malate are much sharper than the signals to their right. These latter signals from vacuolar malate appear to consist of multiple overlapping resonances, rather than a single broad resonance. The spectra of shorter root tips (Fig. 1, B and C) also suggest multiple vacuolar resonances. From the C1 and C4 titration data presented in Figure 4, pH heterogeneity over a range of a few tenths of a pH unit is suggested by the *in vivo* spectrum. Our result concurs with the findings of Kurkdjian *et al.* (10), who inspected the pH of individual vacuoles of cultured sycamore cells, and showed that vacuolar pH varied from cell to cell, with an approximately Gaussian distribution over the population; most of the vacuoles were within ~0.5 pH unit of each other.

To further test the validity of our assignment of cytoplasmic and vacuolar malate signals, we took advantage of the results of Kime *et al.* (8) and Pfeffer *et al.* (18) who showed that maize root tips can effectively sequester Mn^{2+} in vacuoles, excluding it from the cytoplasm. The paramagnetic manganous ion will greatly broaden resonances of nearby molecules, often to the point of invisibility, particularly if they are anions. This phenomenon is illustrated in Figure 5. Compared to 2 mm root tips (Fig. 5A), ^{31}P-NMR spectra of 12 mm root tips (Fig. 5B) show a much stronger vacuolar Pi resonance relative to signals from cytoplasmic phosphates. The signal from

vacuolar Pi of long root tips is selectively reduced on exposure to low concentrations (0.2 mM) of $MnCl_2$ (Fig. 5C); the cytoplasmic resonances are unaffected. Complete suppression of the vacuolar Pi signal required millimolar concentrations of Mn^{2+}, similar to those used in the studies mentioned above (8, 18). ^{13}C-NMR spectra of 12 mm root tips treated with $KH^{13}CO_3$ in the presence of 0.2 mM $MnCl_2$ show greatly reduced signals from vacuolar malate, while the cytoplasmic malate signals are essentially unchanged (Fig. 6). Enzymic analysis of root tip extracts showed that the $MnCl_2$ treatment did not inhibit the synthesis of malate, only its visibility in the NMR experiment. The $MnCl_2$ treatment clearly suppresses the vacuolar malate signals (Fig. 6) more than the vacuolar ^{31}Pi signal (Fig. 5). Two potential explanations for this difference may be offered. First, Mn^{2+} may be taken up principally by the outer cells of the root apices. If vacuolar Pi is distributed throughout the tissue, and if the malate synthesized using exogenously supplied $H^{13}CO_3^-$ occurs predominantly in the outer cells of the root tips, the signals from malate would be suppressed more than those from vacuolar Pi. Second, assuming Mn^{2+}, malate, and Pi are distributed in vacuoles more or less uniformly throughout the tissue, Mn^{2+} would be expected to interact more strongly with the divalent malate anion than with monovalent Pi, as occurs at pH ~5.3, and so suppress the signal from malate more effectively.

Sequential ^{13}C-NMR spectra of 2 mm root tips during $KH^{13}CO_3$ treatment show that malate accumulates first in the cytoplasm, reaching a fairly constant level there after ~1 h (Figs. 7 and 8). In contrast, signals from vacuolar malate appear after a lag of ~30 min and continue to increase significantly during the latter part of the experiment (Fig. 8). Thus, the proportion of newly synthesized malate that is partitioned into vacuoles progressively increases during $KH^{13}CO_3$ treatment. Maize root tips exhibit high carboxylation and decarboxylation activity (14, 27). For example, Ting and Dugger (27) found that malate in 2 cm maize root tips labeled by a 2 h $NaH^{14}CO_3$ treatment showed exponential decarboxylation, with a time constant of ~30 min. Such data suggest that newly synthesized ^{13}C-malate should have largely equilibrated with the preexisting ^{12}C-malate pool within ~1 h after labeling began. With this assumption, a cytoplasmic volume that is 65% of the total cell volume (25), measurements of total malate and the results in Figure 8, we estimate the concentration of malate in the cytoplasm of 2 mm root tips during $KH^{13}CO_3$ treatment (Table I). These estimated concentrations are larger than the maximum cytoplasmic concentration possible at the beginning of the experiment; the initial malate content is ~3 μmol/g fresh weight, so that if all is in the cytoplasm, the concentration would be ~4.6 mM. Hence, the concentration of cytoplasmic malate appears to increase during $KH^{13}CO_3$ treatment, a result consistent with the observation that, as total tissue malate increases, most of the malate synthesized in the first hour is located in the cytoplasm (Figs. 7A, 8). If malate synthesis occurs predominantly in the outermost cells of the root tips, as was suggested above, changes in cytoplasmic malate would be greater in these cells.

Potential biochemical consequences of a rise in the level of cytoplasmic malate include, on the one hand, stimulation of reactions that remove cytoplasmic malate—decarboxylation via respiration (11) or action of malic enzyme (27), and transport into the vacuole (6). On the other, inhibition of reactions that form malate—via PEP carboxylase (16, 27) or malic enzyme (1, 9) (a possibility generally dismissed)—may occur. *In vitro*, the rates of each of these reactions can be shown to exhibit a dependence on the concentration of malate. We anticipate that ^{13}C-NMR will be useful in determining how the processes of malate metabolism and transport are affected by cytoplasmic malate levels *in vivo*.

ACKNOWLEDGMENTS

We thank Dr. H. Beevers for criticism during the preparation of this manuscript.

LITERATURE CITED

1. **Davies DD** (1984) The co-ordination and integration of metabolic pathways. *In* JM Palmer, ed, The Physiology and Biochemistry of Plant Respiration. Cambridge University Press, Cambridge, pp 159–170
2. **Dry IB, Bryce JH, Wiskich JT** (1987) Regulation of mitochondrial respiration. *In* DD Davies, ed, The Biochemistry of Plants, Vol 2. Biochemistry of Metabolism. Academic Press, New York, pp 213–252
3. **Ferrige AG, Lindon JE** (1978) Resolution enhancement of FT NMR through the use of a double exponential function. J Magn Reson **31:** 337–340
4. **Gerhardt R, Heldt HW** (1984) Measurement of subcellular metabolite levels in leaves by fractionation of freeze-stopped material in nonaqueous media. Plant Physiol **75:** 542–547
5. **Gutmann I, Wahlefeld AK** (1974) L-(−)-Malate determination with malate dehydrogenase and NAD. *In* Methods of Enzymatic Analysis, Ed 2. Academic Press, New York, pp 1585–1589
6. **Heldt HW, Flügge UI** (1987) Subcellular transport of metabolites in plant cells. *In* DD Davies, ed, The Biochemistry of Plants, Vol 12. Physiology of Metabolism. Academic Press, New York, pp 49–86
7. **Johnson HS, Hatch MD** (1969) The C_4-dicarboxylic acid pathway of photosynthesis: identification of intermediates and products and quantitative evidence for the route of carbon flow. Biochem J **114:** 127–134
8. **Kime MJ, Loughman BC, Ratcliffe RG** (1982) The application of ^{31}P nuclear magnetic resonance to higher plant tissue. II. Detection of intracellular changes. J Exp Bot **33:** 670–681
9. **Krebs HA** (1973) Pyridine nucleotides and rate control. Symp Soc Exp Biol **27:** 299–318
10. **Kurkdjian A, Barbier-Brygoo H, Manigault J** (1984) Distribution of vacuolar pH values within populations of cells, protoplasts and vacuoles isolated from suspension cultures and plant tissues. Physiol Veg **22:** 193–198
11. **Lance C, Rustin P** (1983) The central role of malate in plant metabolism. Physiol Veg **22:** 625–641
12. **Lips SH, Beevers H** (1966) Compartmentation of organic acids in corn roots. I. Differential labeling of two malate pools. Plant Physiol **41:** 709–712
13. **Lips SH, Beevers H** (1966) Compartmentation of organic acids in corn roots. II. The cytoplasmic pool of malic acid. Plant Physiol **41:** 713–717
14. **MacLennan DH, Beevers H, Harley JL** (1963) Compartmentation of acids in plant tissues. Biochem J **89:** 316–327
15. **Martin F** (1985) Monitoring plant metabolism by ^{13}C, ^{15}N and ^{14}N nuclear magnetic resonance spectroscopy. A review of the applications to algae, fungi and higher plants. Physiol Veg **23:** 463–490
16. **O'Leary MH** (1982) Phosphoenolpyruvate carboxylase: an enzymologist's view. Annu Rev Plant Physiol **33:** 297–315
17. **Osmond CB, Holtum JAM** (1981) Crassulacean acid metabolism. *In* MD Hatch, NK Boardman, eds, The Biochemistry of Plants, Vol 8. Photosynthesis. Academic Press, New York, pp 283–338

18. **Pfeffer PE, Tu S-I, Gerasimowicz WV, Cavanaugh JR** (1986) *In vivo* ^{31}P NMR studies of corn root tissue and its uptake of toxic metals. Plant Physiol **80:** 77–84
19. **Roberts JKM** (1986) *In* HF Linskens, JF Jackson, eds, Nuclear Magnetic Resonance, Springer-Verlag, Berlin, pp 43–59
20. **Roberts JKM, Jardetzky O** (1981) Monitoring of cellular metabolism by NMR. Biochim Biophys Acta **639:** 53–76
21. **Roberts JKM** (1987) NMR in plant biochemistry. *In* PK Stumpf, EE Conn, eds, The Biochemistry of Plants, Vol 13. Methodology. Academic Press, New York, pp 181–227
22. **Roberts JKM, Ray PM, Wade-Jardetzky N, Jardetzky O** (1980) Estimation of cytoplasmic and vacuolar pH in higher plant cells by ^{31}P NMR. Nature **283:** 870–872
23. **Roberts JKM, Wemmer D, Ray PM, Jardetzky O** (1982) Regulation of cytoplasmic and vacuolar pH in maize root tips under different experimental conditions. Plant Physiol **69:** 1344–1347
24. **Splittstoesser WE** (1966) Dark CO_2 fixation and its role in the growth of plant tissue. Plant Physiol **41:** 755–759
25. **Steer WM** (1981) Understanding Cell Structure. Cambridge University Press, Cambridge, pp 77–84
26. **Stidham MA, Moreland DE, Siedow JN** (1983) ^{13}C Nuclear magnetic resonance studies of crassulacean acid metabolism in intact leaves of *Kalanchoë tubiflora*. Plant Physiol **83:** 517–520
27. **Ting IP, Dugger MW Jr** (1967) CO_2 metabolism in corn roots. I. Kinetics of carboxylation and decarboxylation. Plant Physiol **42:** 712–718